Supplemental Information

LEPTIN FACILITATES REPRODUCTION THROUGH NEURONAL NITRIC OXIDE SIGNALING IN THE HYPOTHALAMIC PREOPTIC REGION

Nicole Bellefontaine[1,2], Konstantina Chachlaki[1,2], Jyoti Parkash [1,2], Charlotte Vanaker[1,2], William Colledge[3], Xavier d'Anglemont de Tassigny[3], John Garthwaite[5], Sebastien G Bouret[1,2,6],Vincent Prevot[1,2]

Supplemental Results

Computer modeling of NO signaling in the median preoptic nucleus before and after leptin treatment

nNOS neurons in the preoptic region in the presence of leptin were modeled on the basis of a stereological analysis of nNOS neurons in sections of the median preoptic nucleus. From measurements made in 55 μm-thick tissue sections, the mean diameter of nNOS neurons was 15 ± 0.3 μm and there were 80 ± 3 of these cells per 24000 μm^2. After applying Abercrombie's correction (1), the packing density comes to 4.76 x 10^4 nNOS neurons/mm^3. To simulate this tissue, nNOS neurons were modeled as a 3-dimensional cubic array of spheres (9x9x9), each 15 μm in diameter, and having the same nearest-neighbour spacing (28 μm) that would exist if the nNOS neurons were similarly packed. [With this geometry, the distance to the nearest neighbour is given by (packing density)$^{-1/3}$; (2)]. Because active nNOS is presumed to be associated with the cell membrane, NO was emitted from the surfaces of the spheres. Diffusion from a continuous spherical surface source is given by Equation 10.4.10 of Carslaw and Jaeger (3). The equation was modified to incorporate the x-, y- and z-coordinates and to sum the contributions of all the spheres located within these coordinates (*n* in each plane). The resulting equation was:

$$[NO](x,y,z,t) = \frac{1}{10^3 N_{av}} \sum_{a=0}^{n-1} \sum_{b=0}^{n-1} \sum_{c=0}^{n-1} \left[\frac{Q}{8\pi R r' \sqrt{\pi D}} \int_0^t \frac{1}{\sqrt{t-t'}} \exp\left[-\frac{(R-r')^2}{4D(t-t')} - \lambda(t-t') \right] \right.$$

$$\left. - \exp\left[-\frac{(R+r')^2}{4D(t-t')} - \lambda(t-t') \right] \right] dt'$$

where $R = \sqrt{(x-x_a')^2 + (y-y_b')^2 + (z-z_c')^2}$

and, with the units given in parentheses, *[NO]* = NO concentration (M), N_{av} = Avagadro's number (molecules/mole), *Q* = rate of NO release (molecules/s), *r'* is the radius of the spherical source surface (m), *D* = NO diffusion coefficient (m^2/s), *t* = time (s), λ = NO

inactivation rate constant (s^{-1}), x,y,z are distances in the 3 dimensions (m), x'_a, y'_b and z'_c are the coordinates of the *n* sources in each dimension, indexed (*a,b* and *c*) to reside at regularly-spaced intervals.

A range of values for the rate of NO inactivation was considered (λ = 1-150 s^{-1}) and, to ensure steady-state conditions even at the slowest rate (λ = 1 s^{-1}), the sources were set to run for 10 s. The resultant NO concentration profile is proportional to the rate of NO release (*Q*), the value of which was selected on the basis of the measured NO synthase activity in the hypothalamus, namely15 nmol/min/g tissue (4). Assuming 1 ml/g tissue, this activity corresponds to 3.46 x 10^{-15} mol/s for the array volume, or 2.84 x 10^6 NO molecules/s for each constituent sphere. Given that brain tissue has a relatively small extracellular space [20 % of the volume, (5)], the NO diffusion coefficient (D) was taken to be its intracellular value [8.48 x 10^{-10} m^2/s; (6)]. The equation was solved using the "Adaptive" integrator in Mathcad 14 (Parametric Technology Corp., Needham, MA, USA).

A key determinant of the amplitude and spread of NO signals is the rate of NO inactivation and we have considered a range of NO inactivation rate constants (λ), from 1 s^{-1}, which is approximately the value expected if loss of NO was solely through interaction with hemoglobin in the microcirculation (7), up to 150 s^{-1}, which is the value deduced for slices of cerebellum at subnanomolar NO concentrations (8). When λ = 1 s^{-1} the resulting NO concentration is high (approximately 200 nM) and roughly uniform over the lattice (Supplemental Figure 2A), whereas with higher rates of inactivation, the profiles of NO over each sphere become progressively smaller and more distinct (see Supplemental Figure 2B top panel for λ = 100 s^{-1}). Even at high rates of inactivation, however, appreciable intercellular NO concentrations are predicted to exist. For example, with λ = 100 s^{-1}, the steady-state intercellular concentrations at their lowest points (troughs) reach 1.3 nM, which is about 15 % of the concentration found at the NO-emitting spherical surfaces.

In order to simulate the pre-leptin situation, the number of sources was reduced, while keeping the overall dimensions of the lattice the same. With a 7x7x7 lattice (containing about half the number of NO-emitting spheres), trough NO concentrations with $\lambda = 100$ s^{-1} are predicted to be reduced to about 15 % of those found in the fully active lattice, although the concentrations at the sources are unaltered (Supplemental Figure 2B, second panel). With further reductions in the density of spheres, the trough NO concentrations become increasingly negligible (Supplemental Figure 2B, lower panels) provided that the rate of NO inactivation is reasonably high (Supplemental Figure 1A).

From the relationship between the trough NO concentrations, the density of spheres, and the NO inactivation rate (Supplemental Figure 2C), it can be concluded that, providing the numbers of active nNOS neurons in the tissue in the pre-leptin situation are half or less of the numbers in the fully active population (post-leptin), and provided that the rate of NO inactivation is relatively high, leptin would augment the NO concentration in the vicinity of the intermingled GnRH neurons by at least 10-fold.

Parenthetically, we also note that the values of the computed NO concentrations arrived at by assuming a rate of NO synthesis based on the hypothalamic NOS activity, together with a high rate of NO inactivation, are very similar to the concentrations (low nM) deduced from measurements of NO release to exist within the nNOS-rich regions of cerebellar slices following stimulation with NMDA, concentrations that also cohere with the measured cerebellar nNOS activity (9).
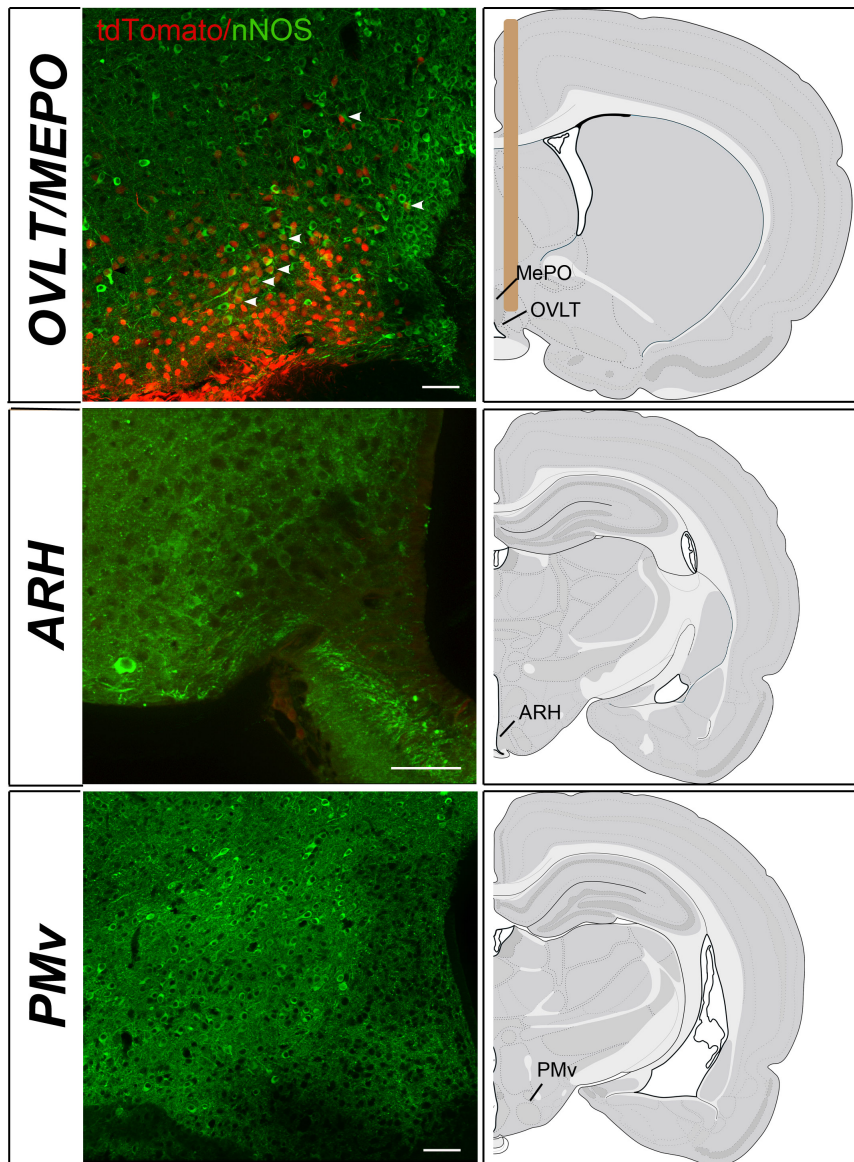
Supplemental Figures
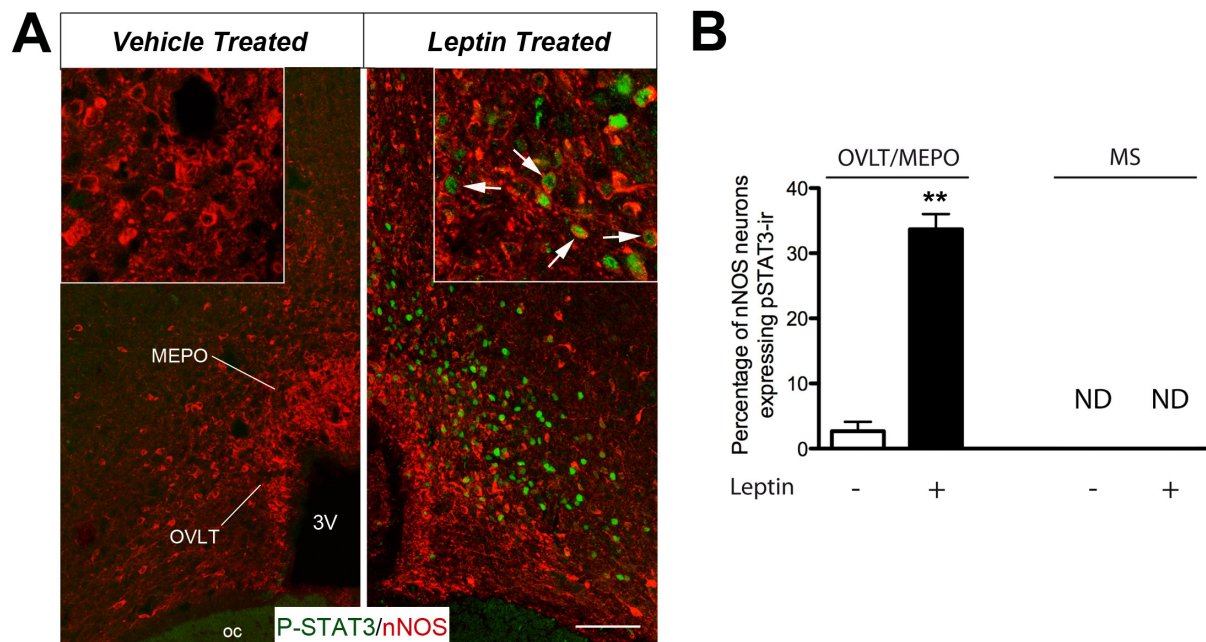
Supplemental Figure 1. Intraperitoneal injection of leptin promotes STAT3 phosphorylation in nNOS neurons in the preoptic region, but not in the medial septum (MS). (A) Coronal section of the preoptic region showing a marked increase in P-STAT3 expression (green) in leptin *vs.* vehicle treated diestrous mice at the level of the organum vasculosum of the lamina terminalis (OVLT) and the medial preoptic area (MePO) where numerous nNOS-immunoreactive neurons reside (red). Arrows in inset show double-labelled neurons. 3V, third ventricle; oc, optic chiasm. Scale bar: 100 μm (30 μm in insets). (B) Graphs represent the proportion of nNOS neurons expressing P-STAT3 immunoreactivity in the OVLT/MePO and MS in leptin (+) or vehicle (-) treated animals. N.D.: not detected. ** P < 0.01 *vs.* vehicle.
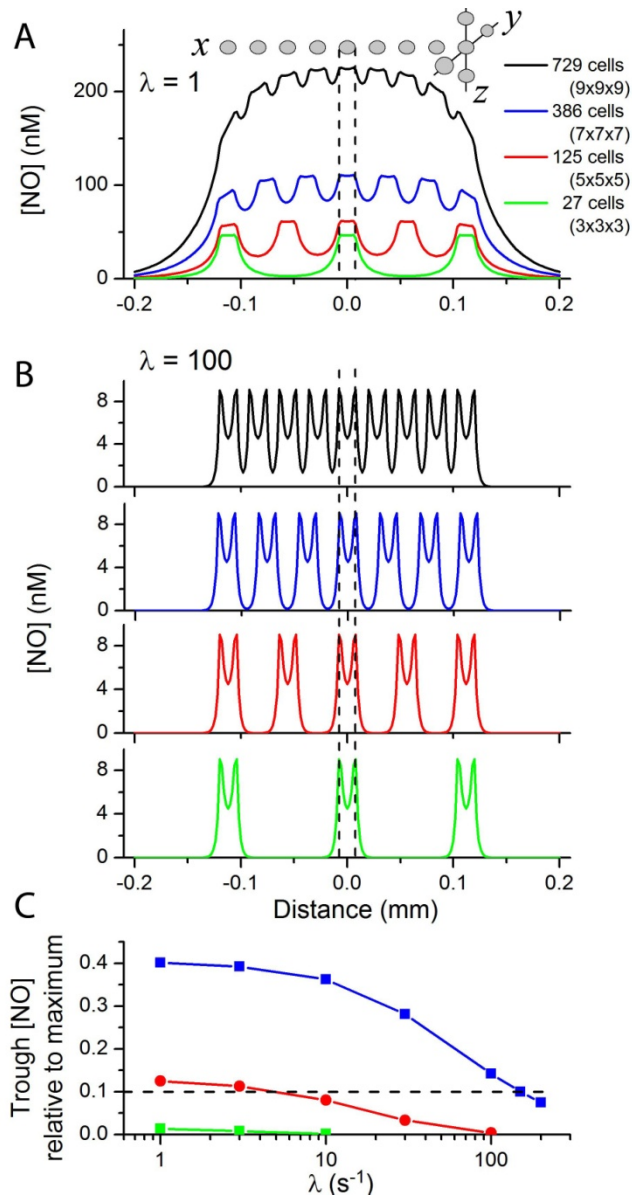
Supplemental Figure 2. Model of NO signaling in the preoptic region of the hypothalamus. A and B show the computed profiles of steady-state NO concentrations across the center of a cubic array of spherical surface sources. The 9x9x9 array is depicted diagrammatically at the top of panel A and the vertical broken lines indicate the boundaries of the central sphere. Different numbers of active spheres are considered (color-coded as in the legend to panel A) with NO inactivation rate constants (λ) of 1 s^{-1} (A) and 100 s^{-1} (B). In C, the lowest NO concentrations found in the inter-sphere region (the troughs) are expressed relative to the values found when all spheres in a 9x9x9 array are active, at different values of λ. The horizontal broken line indicates trough concentrations that are 10 % of those found in the 9x9x9 array. The color-coding is as in A and B.

Supplemental Figure 3. Representative images showing Tomato expression (red) in nNOS (green)-immunoeactive neuons (arrowheads) in the OVLT/MEPO, but not the ARH and PMv of *dtTomato*[loxP/+] mice in which the tat-cre recombinant protein has been infused into the preoptic region. Scale bars: 50 μm.
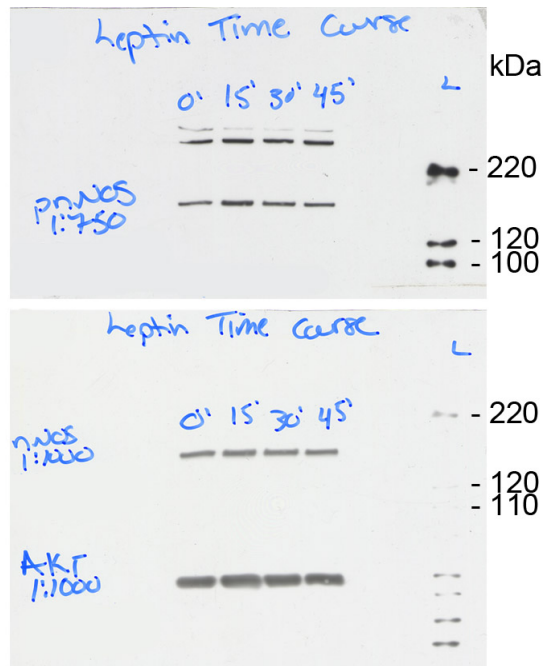
Figure 1 A

Supplementary Figure 4. Full-length photographs of the western blots presented in Figure 1A.

Supplemental Experimental Procedures

Immunofluorescent stainings

Immunohistochemistry of P-STAT3 and nNOS. Mice were given a lethal overdose of chloral hydrate (400mg/kg) then perfused transcardially with cold saline (0.9%) followed by cold 2% paraformaldehyde in 0.1M sodium phosphate buffer (PB) pH 7.4. Brains were collected immediately after perfusions and post-fixed for 2 hours in a 20% sucrose- 2% paraformaldehyde solution. Following postfixation brains were cryoprotected in 20% sucrose-KPBS 0.02M solution overnight, then imbedded in OCT, flash frozen, and stored at -80°C until further processing. Coronal sections were taken at 30um through the preoptic area directly onto Superfrost slides and stored in antifreeze at -20°C. Sections were washed 4 times in KPBS 0.02M for 15minutes each. Sections were then treated with a 0.5% H_2O_2 +0.5% NaOH solution in KPBS for 20minutes at room temperature. The sections were washed 5 times for 5 minutes each in KPBS. Sections were then treated with 0.3% glycine in KPBS for 10 minutes at room temperature and then washed 5 times for 5 minutes each in KPBS. Following the washes, the slides were treated with a 0.03% SDS solution in KPBS for 10 minutes at room temperature and then washed 5 times 5 minutes in KPBS. Sections were incubated in blocking solution (4% NDS + 0.4% Triton X-100 +1% BSA in KPBS 0.02M) for 90 minutes. Then sections were then incubated in rabbit anti-P-STAT3 (Tyr705) (Cell Signaling) 1/1000 and sheep anti-nNOS (generous gift from Dr. P. C. Emson (Medical Research Council, Laboratory for Molecular Biology, Cambridge, UK) in a KPBS 0.02M solution containing 1% NGS + 0.4% Triton X-100 + 1% BSA for 48 hours at 4°C. After the incubation in the primary antibody, sections were rinsed with KPBS 0.02M 8 times for 5 minutes each. The sections were then incubated in secondary antibody donkey anti-rabbit Alexa-568 (Invitrogen) and donkey anti-sheep Alexa-488 (Invitrogen) for 2 hours at room temperature. Sections were washed in KPBS 5 times for 5 minutes each then counterstained with bis-benzamide for 3 minutes and washed 2 times for 5 minutes and coverslipped with 65% glycerol in KPBS 0.02M.

Immunofluorescence for pnNOS and nNOS. Mice were given a lethal overdose of chloral hydrate (400mg/kg) then perfused transcardially with cold saline (0.9%) followed by cold 4% paraformaldehyde in 0.1M PB pH 7.4. Brains were collected after perfusions and post-fixed for 4 hours in 4% paraformaldehyde followed by cold PB 0.1M. The following day brains were sliced coronally to collect free-floating sections using a Vibratome V1200ST at 50um and were immediately processed for immunohistochemistry. Sections were washed 3 times for 15 minutes each in PB 0.1M and then incubated in blocking solution (5% NDS + 0.3% Triton X-100 in PB 0.1M) for 1 hour at room temperature. Sections were then incubated for 72hours at 4°C in primary rabbit anti-pnNOS (Thermoscientific) and sheep anti-nNOS. Sections were washed 3 times for 5 minutes in PB 0.1M and then incubated in donkey anti-rabbit biotin (1:500; Jackson Laboratories) for 1 hour at room temperature. The sections were then washed and incubated in streptavidin Alexa 488 (1/400; Invitrogen) and donkey anti-sheep Alexa 568 (1/400; Invitrogen). Sections were washed, mounted, and coverslipped with 65% glycerol in PB 0.1M.

Western blot analyses

Protein extraction. The preoptic region was dissected from each animal and protein extracted for western blotting as described previously. Briefly, mice were killed by decapitation following treatment. After the rapid removal of the brain, the meninges and optic chiasm were removed and the preoptic region was dissected under a binocular magnifying glass with the Wecker scissors (Moria, France). The external limits for this dissection were: laterally, the external border of the medial preoptic area and dorsally, the internal border of the anterior commissures. Anteroposteriorly, the dissected region was comprised between the atlas levels 16 and 20 of the Swanson Atlas (10). After dissection, each fragment was placed in a microcentrifuge tube, snap frozen in liquid nitrogen and stored at -80°C.

Protein extracts were prepared from each preoptic region sample in 200 µl of lysis buffer (25 mM Tris, pH 7.4, β-glycerophosphate, 1.5 mM EGTA, 0.5 mM EDTA, 1 mM sodium pyrophosphate, 1 mM sodium orthovanadate, 10 µg/ml leupeptin and pepstatin A, 10 µg/ml

apoprotinin, 100 µg/ml PMSF, and 1% Triton-X100) by homogenization of the fragments through 22 and 26 gauge needles in succession. Tissue lysates were cleared by centrifugation at 14000 rpm for 15 min at 4°C. Protein content was determined using the Bradford method (Bio-Rad, Hercules, CA) and equal amount of protein were mixed with 4X sample buffer (Invitrogen). Samples were boiled for 5 min and stored at -80°C until use.

Immunoblot. Samples were reboiled for 5 min after thawing and electrophoresed for 75 min at 150 V in 8-12% Tris-acetate polyacrylamide gels according to the protocol supplied with the NuPAGE system (Invitrogen). After size fractionation, the proteins were transferred onto 0.2 µm pore-size polyvinylidene difluoride membranes (LC2002; Invitrogen) in the blot module of the NuPAGE sytem (Invitrogen) for 75 min at RT. Membranes were blocked for 1 h in blocking buffer [TBS with 0.05% Tween 20 (TBST) and 5% nonfat milk] at RT, and incubated overnight at 4°C with primary rabbit anti-pnNOS (Thermoscientific) diluted in blocking buffer. Membranes were washed four times with TBST the following day before being exposed to HRP-conjugated secondary antibodies diluted in blocking buffer for 1 h at RT. Immunoreactions were visualized using the ECL detection kit (NEL101; PerkinElmer, Boston, MA). Immunoblots were scanned using a desktop scanner (Epson Expression 1680 PRO) and Adobe Photoshop, and band intensities were determined using ImageJ software (NIH, Bethesda).

Fasting-induced suppression of LH levels

Vaginal smears were taken from adult female mice for two complete estrous cycles prior to the fast. On the day of diestours I, female mice were placed under food deprivation for 24 hours to disrupt fertility. At the beginning of the light cycle (7H30) food was removed and subsequently treated with bidaily injections of the NOS inhibitor L-NAME (50mg/kg, i.p.) or a control (saline) one hour prior to leptin (3mg/kg, i.p.) or vehicle injections. The timing of the bidaily injections are as follows: L-NAME or the control where administered at 8H30 and 18H30, while leptin or vehicle were administered at 9H30 and 19H30. Food was returned at 7H30 exactly 24 hours following the initial food deprivation. Mice were sacrificed on the

evening of the predicted proestrous precisely at 19H30 (lights-off) and blood was collected for later analyses.

Stereotaxic surgery

Acute stereotaxic surgery and peripheral leptin treatment. On the day of diestrous I, mice were deeply anesthetized using 4% isoflurane to O_2 then transferred to the stereotaxic apparatus and anesthetized with 1.5-2.5% isoflurane to O_2 for the duration of the surgery with constant monitoring of temperature and breathing rate. Mice were administered L-NAME (5mM) or sterile saline into the POA (coordinates: +0.5mm bregma, -0.5mm lateral, -5.3mm dorsal-ventral) via a Hamilton syringe at a rate of 50nl/minute. The syringe was left untouched for 3 minutes following injection. Generally, mice were fully mobile 5 minutes following the removal of the anesthesia and were allowed to recover under a heat lamp 15 minutes prior to leptin treatment. Leptin was administered intraperitoneally 15 minutes following surgery and sacrificed by live decapitation 15 minutes following the injection. Blood was collected for LH level analysis and the brain removed for correct placement of the syringe.

Chronic L-NAME Infusion and Daily Peripheral Leptin Treatment for 28 Days. Cannulae (Plastics One) were attached via a catheter to a 14-day osmotic minipump (Alzet; model 2002). The minipumps contained either vehicle (sterile saline 0.9%) or L-NAME (5mM) and were primed overnight in sterile saline at 37°C. Lep[ob/ob] mice were anesthetized using a 2% Avertin (Sigma) solution. The cannula was implanted into the POA as described above and the minipump placed into the subcutaneous space in the back. Mice were allowed to recover for 24 hours prior to the start of peripheral leptin administration. Lep[ob/ob] mice were weighed and administered leptin (3mg/kg) once daily at the end of the light cycle for 28 days. As the duration of the minipump was 14 days a second surgery was required to change the minipump to continue the treatment. On the morning of the 14th day of the leptin regime, the minipump was changed by applying a local anesthetic directly on the back surrounding the

area of the minipump before an incision was made. Mice were allowed to recover under a heat lamp for the afternoon prior to the daily leptin injection.

Supplemental references

1. Abercrombie M. Estimation of nuclear population from microtome sections. *The Anatomical record.* 1946;94:239-47.
2. Rusakov DA, Kullmann DM, and Stewart MG. Hippocampal synapses: do they talk to their neighbours? *Trends in neurosciences.* 1999;22(9):382-8.
3. Carslaw HS, and Jaeger JC. *Conduction of Heat in Solids.* Oxford: Clarendon Press; 1986.
4. Salter M, Duffy C, Garthwaite J, and Strijbos PJ. Substantial regional and hemispheric differences in brain nitric oxide synthase (NOS) inhibition following intracerebroventricular administration of N omega-nitro-L-arginine (L-NA) and its methyl ester (L-NAME). *Neuropharmacology.* 1995;34(6):639-49.
5. Sykova E, and Nicholson C. Diffusion in brain extracellular space. *Physiological reviews.* 2008;88(4):1277-340.
6. Liu X, Srinivasan P, Collard E, Grajdeanu P, Zweier JL, and Friedman A. Nitric oxide diffusion rate is reduced in the aortic wall. *Biophysical journal.* 2008;94(5):1880-9.
7. Santos RM, Lourenco CF, Pomerleau F, Huettl P, Gerhardt GA, Laranjinha J, and Barbosa RM. Brain nitric oxide inactivation is governed by the vasculature. *Antioxidants & redox signaling.* 2011;14(6):1011-21.
8. Hall CN, and Garthwaite J. Inactivation of nitric oxide by rat cerebellar slices. *The Journal of physiology.* 2006;577(Pt 2):549-67.
9. Wood KC, Batchelor AM, Bartus K, Harris KL, Garthwaite G, Vernon J, and Garthwaite J. Picomolar nitric oxide signals from central neurons recorded using ultrasensitive detector cells. *The Journal of biological chemistry.* 2011;286(50):43172-81.
10. Swanson LW. *Structure of the rat brain.* Amsterdam: Elsevier Science Publishers; 2004.